

Valid predictions of group-level random effects

Nicholas Syring^{‡,*}, Fernando Miguez[†], Jarad Niemi[‡]

February 7, 2022

Abstract

Gaussian linear models with random group-level effects are the standard for modeling randomized experiments carried out over groups, such as locations, farms, hospitals, or schools. Group-level effects can be summarized by prediction intervals for group-level means or responses, but the quality of such summaries depends on whether the intervals are valid in the sense they attain their nominal coverage probability. Many methods for constructing prediction intervals are available—such as Student- t , bootstrap, and Bayesian methods—but none of these are guaranteed to be valid, and indeed are not valid over a range of simulation examples. We propose a new method for constructing valid predictions of group-level effects based on an inferential model (IM). The proposed prediction intervals have guaranteed finite-sample validity and outperform existing methods in simulation examples. In an on-farm agricultural study the new IM-based prediction intervals suggest a higher level of uncertainty in farm-specific effects compared to the standard Student- t based intervals, which are known to undercover.

Keywords and phrases: Inferential model; Meta-analysis; Prediction interval; Random effect.

1 Introduction

One-way, random-effects ANOVA with a Gaussian error term is the standard for modeling treatment effects over sampled groups. Common applications include meta-analyses of treatment-efficacy, and on-farm agricultural trials. Traditionally, inferences based on these models have mainly concerned the overall treatment effect averaged over observed groups. However, from the point of view of a group-level actor the group-level mean treatment effect is most relevant. As discussed in Altman and Krzywinski (2013) and Altman and Krzywinski (2018), practitioners may struggle to recognize the differences in variability between population-, group-, and individual-level parameters, and do not always choose the appropriate inference method for the parameter of interest. As pointed out in Higgins et al. (2009) and Inthout et al. (2016), confidence intervals for overall treatment effect are often used to make inferences on group-level effects, but these intervals systematically underestimate variability at the group level.

*Corresponding author: nsyring@iastate.edu

[†]Department of Agronomy, Iowa State University

[‡]Department of Statistics, Iowa State University

Prediction intervals for group-level means—and not confidence intervals for the overall mean—are appropriate for group-level inferences. Higgins et al. (2009) proposes a Student’s t -based prediction interval for group-level means, but both Inthout et al. (2016) and Partlett and Riley (2016) point out that in applications exhibiting very low between-group variability in response these prediction intervals are not valid. In an experiment involving many on-farm agricultural trials Laurent et al. (2020) observed low between-farm variability in response relative to within-farm variability, and found that Student’s t -based prediction intervals for farm-level mean treatment effect under-covered.

Since standard prediction intervals perform poorly in practically relevant examples, the question is: what alternative method reliably produces valid prediction intervals? Both bootstrap-based predictions and Bayesian posterior-predictive credible intervals are reasonable candidate methods. However, we find neither of these out-perform Student’s t -based intervals in simulation examples. Instead, we propose prediction intervals based on an *inferential model* (IM) following the works of Cella and Martin (2020); Martin and Lingham (2016); Martin and Liu (2015b). General IM theory guarantees our prediction intervals will be valid for any sample size and any level of between-group variability. Besides being theoretically grounded, the IM approach holds up in simulation experiments, performing better than Student’s t -based intervals, bootstrap methods, and Bayesian approaches. And, in an application to an on-farm agricultural trial, our IM-based predictions suggest greater group-level variability than Student’s t -based prediction intervals, which are known to under-cover.

The paper is laid out as follows. Section 2 introduces our model with a random group-level effect along with our notation and an explanation of various quantities of interest. The IM framework is unfamiliar to most readers, so we provide a brief introduction to IM concepts in Section 3, including a precise definition of what it means for prediction intervals to be valid. The general method for constructing an IM is challenging to apply to our model. To provide a gentle introduction to IM construction we illustrate IM prediction for independent and identically distributed (iid) normal responses in Section 4. Section 5 presents the IM construction and prediction intervals for group means and individual responses based on our Gaussian linear model. Some technical details related to the construction are deferred to Appendix A. Section 6 provides an overview of our extensive simulation study comparing the IM approach to several competing methods, and additional simulation results are included in Appendix B. Section 7 applies our proposed IM prediction method to the on-farm agricultural experiment data from Laurent et al. (2020) which exhibits low between-group variance. Section 8 provides concluding remarks. Codes for implementing our approach are freely available in a downloadable R package at <https://github.com/nasyring/impred>.

2 Gaussian linear model for random group effects

The Gaussian linear model for modeling random group-level effects can be written

$$y_{ij} = \mu + \alpha_i + \varepsilon_{ij}, \quad \varepsilon_{ij} \stackrel{iid}{\sim} N(0, \sigma^2), \quad \alpha_i \stackrel{iid}{\sim} N(0, \sigma_a^2)$$

where α_i and ε_{ij} are mutually independent and y_{i1}, \dots, y_{in_i} denote the n_i observations in group i for groups $i = 1, \dots, I$; μ denotes the overall treatment effect; and, σ_a^2 and

σ^2 denote the between- and within-group variance components, respectively. The total sample size is $n = \sum_{i=1}^I n_i$. In vector-matrix notation the model may be written

$$Y^n = \mu \mathbf{1} + (\sigma_a^2 Z Z^\top + \sigma^2 I_n)^{1/2} W, \quad (1)$$

where $Y^n = (y_{11}, \dots, y_{In_I})^\top$ is the $n \times 1$ vector of responses; $\mathbf{1}$ is the $n \times 1$ vector of ones; Z is the design matrix of ones and zeroes indicating the group memberships of y_{ij} 's, and has form $Z = [Z_1, \dots, Z_I]$ where $Z_{ij} = 1$ if $j \in \left[1 + \sum_{\ell=1}^{i-1} n_\ell, \sum_{\ell=1}^i n_\ell\right]$ for $i = 1, \dots, I$ and $Z_{ij} = 0$ otherwise; I_n is the $n \times n$ identity matrix; and, $W \sim N_n(0, I_n)$.

We denote the group-level mean effects by $\theta_i := \mu + \alpha_i$. For example, in a meta-analysis application the I groups represent I clinical studies of the same treatment and the parameters θ_i , $i = 1, \dots, I$ represent the study-specific treatment effects. An important inferential question is: what range of treatment effects can be expected in a new study? The corresponding parameter of interest is the true mean of a new/unobserved group, written $\theta^* := \mu + \alpha^*$, where $\alpha^* \sim N(0, \sigma_a^2)$. A related question is: what range of sample treatment effects can be expected in a new study of k individuals? The corresponding parameter of interest is denoted \bar{Y}_k^* —the sample mean response of k individuals sampled from a new group.

In Section 7 we apply (1) to an on-farm agricultural trial. In that setting the I groups represent I Iowa farms that experimented with the use of a fungicide to improve soybean yields. The key research question concerns the expected yields at a new farm—the most important question from the perspective of an Iowan farmer reading about the study and weighing whether to use the fungicide in the future. Answering this question requires valid prediction of θ^* and/or \bar{Y}_k^* .

3 Valid predictive inference

Below we define what it means for predictions of θ^* and \bar{Y}_k^* to be “valid”. This requires a brief overview of the IM framework for valid predictive inference presented in Cella and Martin (2020) and Martin and Liu (2020).

Let P denote the joint distribution of (Y^n, θ^*) , and let $C_\alpha(y^n)$ denote a $100(1 - \alpha)\%$ prediction interval for θ^* based on data $Y^n = y^n$. $C_\alpha(y^n)$ is valid for predicting θ^* if

$$P\{\theta^* \in C_\alpha(Y^n)\} \geq 1 - \alpha, \quad \forall \alpha, n, P; \quad (2)$$

and see Cella and Martin (2020) where this property is referred to as “weak validity”. Predictive validity with respect to a prediction interval for a new response Y^* , or the sample mean of k new responses, \bar{Y}_k^* , is defined the same way; simply replace θ^* in (2) by the alternative prediction target.

In the IM framework, valid prediction intervals are a by-product of a so-called valid plausibility function that can be constructed according to the strategy laid out in Cella and Martin (2020). *Plausibilities* are like p-values; they are numbers between 0 and 1 indicating the strength of *assertions* or claims that θ^* or \bar{Y}_k^* belongs to a particular set of values, written, e.g., $\{\bar{Y}_k^* \in A\}$ for $A \subset 2^{\mathbb{R}}$, where $2^{\mathbb{R}}$ denotes the power set of the real numbers, \mathbb{R} . A *plausibility contour* is any function assigning plausibilities to singleton values, written $\pi : \mathbb{R} \mapsto [0, 1]$. Simple examples of a plausibility contour include the

flat contour $\pi(x) = 1$ for $x \in \mathbb{R}$ and the triangular contour $\pi(x) = 1/2 - |x - 1/2|$ for $x \in [0, 1]$, which illustrates that plausibility contours are not equivalent to probability densities or distribution functions. The plausibility contour extended to sets is called a *plausibility function*, written $\bar{\Pi} : 2^{\mathbb{R}} \mapsto [0, 1]$, and defined by $\bar{\Pi}(A) := \sup_{a \in A} \pi(a)$ for any $A \subset 2^{\mathbb{R}}$. When the plausibility contour/function depends on data we indicate the dependence with a subscript n as in π_n and $\bar{\Pi}_n$. Section 4 below provides an example construction of a plausibility contour for predicting the mean of iid normally-distributed responses.

Given a data-dependent plausibility contour $\pi_n(\vartheta)$ for θ^* define a $100(1 - \alpha)\%$ prediction set for θ^* to be the set $\{\vartheta : \pi_n(\vartheta) \geq \alpha\}$. In the present context this set always takes the form of an interval equivalent to the α -cut of $\pi_n(\vartheta)$. That is, slice the graph of $\pi_n(\vartheta)$ at height α and define the lower endpoint of the prediction interval to be the smallest value ϑ with $\pi_n(\vartheta) = \alpha$; likewise, define the upper endpoint of the prediction intervals to be the largest value ϑ with $\pi_n(\vartheta) = \alpha$. It turns out this prediction interval is valid in the sense of (2) if its corresponding plausibility function $\bar{\Pi}_n(\vartheta)$ has the validity property given in (3) below.

A plausibility function $\bar{\Pi}_n$ is valid for predicting θ^* if it is unlikely to assign low plausibility to sets containing θ^* . Writing $\phi = (\mu, \sigma_a^2, \sigma^2)$ for the model parameters, *predictive validity* of $\bar{\Pi}_n(A)$ means that for all n, ϕ, A , and $\alpha \in (0, 1)$,

$$P_{(Y^n, \theta^*)|\phi} \{\bar{\Pi}_n(A) \leq \alpha, \theta^* \in A\} \leq \alpha, \quad (3)$$

where P refers to the joint sampling distribution of (Y^n, θ^*) parametrized by ϕ . Section 5 details our construction of valid plausibility contours for group-level means and for new responses based on the model in (1).

In some applications there are other predictive inferences of interest besides prediction intervals. For instance, a researcher may want a prediction about whether a new group-level mean is greater than some predetermined level, i.e., $\{\theta^* > \vartheta\}$. Higgins et al. (2009) point out that one goal of meta-analysis is to predict whether the effect in a new study will be positive, which can be answered by assigning plausibility to the assertion $\{\theta^* > 0\}$. The notion of validity in (3) above is not limited to prediction intervals; rather, plausibility functions meeting (3) produce both valid prediction intervals in the sense of (2), and valid predictions about general assertions, e.g., $\{\theta^* > 0\}$.

Besides validity we desire predictive inferences to be efficient; for example, if two methods both produce valid prediction intervals, then we generally prefer the method producing the shortest intervals on average. Not much is known about efficiency of IM prediction intervals, but we can say for certain that if the right-hand-side of (3) is smaller than α , say, $\alpha/2$, then $100(1 - \alpha)\%$ prediction intervals for θ^* will have coverage at least $100(1 - \alpha/2)\%$. For this reason, if $\bar{\Pi}_n$ satisfies (3) with equality, then we say the plausibility function is efficient.

4 An illustration of IM prediction

In this section we demonstrate how to construct a valid plausibility contour for predicting a normal random variable $Y^* \sim \mathbf{N}(\mu, \nu^2)$ with unknown mean and variance based on a random sample of size n . This simpler problem provides an illustration for the

general three-step method of IM construction: 1) *associate* the data, prediction, and an auxiliary random variable with a known distribution via an equation; 2) *predict* the auxiliary random variable with a valid plausibility contour π ; and 3) *combine* by pushing the plausibility contour forward through the association equation to determine a data-dependent plausibility contour π_n for the target. For further details, see the alternative construction of IM predictions in Martin and Lingham (2016), and for an extension of IM prediction to nonparametric/misspecified model settings see Cella and Martin (2020) where the authors connect IM and conformal predictions.

The first—and often most challenging—step in the construction is to define an appropriate association, or data-generating equation like that in (1). We can start with the $n + 1$ data-generating equations for the observations and prediction:

$$Y^n = \mu + \nu I_n \Psi^n, \quad Y^* = \mu + \nu \Psi,$$

where $\Psi^n = (\Psi_1, \dots, \Psi_n)^\top$, $\Psi_j \stackrel{iid}{\sim} N(0, 1)$ for $j = 1, \dots, n$, and $\Psi \sim N(0, 1)$, independent from Ψ^n . The idea is to use the association like a system of equations that we can solve to determine the values of the unknown parameters, given the observations and predictions of the auxiliary random variables. In order to yield a unique solution the number of equations in the association should match the dimension of the parameter. For the above association, we have three unknown parameters, (Y^*, μ, ν) , in $n + 1$ equations, so our association includes too many equations. Martin and Liu (2015b) discusses reducing the dimension of associations, and often the first step is to rewrite the association so that it depends on the data only through the minimal sufficient statistic. Further dimension-reduction techniques focus on removing unnecessary associations involving only nuisance parameters, here μ and ν . Using the sample mean \bar{Y}_n and the sample variance S_n^2 we have the three-dimensional association

$$S_n^2 = \frac{\nu^2}{n-1} \chi^2, \quad \bar{Y}_n = \mu + \frac{\nu}{\sqrt{n}} I_n \Psi^n, \quad \text{and } Y^* = \mu + \nu \Psi. \quad (4)$$

And, by solving for μ and ν in the first two displays above and substituting into the third, we obtain

$$Y^* = \bar{Y}_n + T \sqrt{S_n^2 (1 + \frac{1}{n})} =: G_n(T), \quad (5)$$

where $T \sim T_{n-1}$ has a Student t distribution with $n-1$ degrees of freedom. Next, we apply the IM principle of *marginalization* to drop the first two equations in (4) and retain only (5) as our final association. The reasoning is as follows: for any $(Y^*, \bar{Y}_n, T, S_n^2)$ satisfying (5) there is a pair (ν^2, μ) that solve the first two equations in (5). These are free variables that do not carry any information about Y^* , so we may safely ignore/marginalize those two equations.

The next step is to select a valid plausibility contour $\pi(t)$ for predicting the auxiliary random variable T . Many choices of auxiliary plausibility contour are possible, but in order to prove predictive validity of the data-dependent predictive plausibility contour π_n the auxiliary contour $\pi(t)$ should satisfy, for all $\alpha \in (0, 1)$

$$P_T\{\pi(T) \leq \alpha\} \leq \alpha, \quad T \sim T_{n-1}. \quad (6)$$

In other words, $\pi(T)$ is uniformly distributed with respect to $T \sim T_{n-1}$. At least in this example it turns out an optimal choice of $\pi(t)$ is available — one that leads to the most

efficient inferences about Y^* , e.g., tightest valid prediction intervals — and it is given by

$$\pi(t) = P_T\{f(T) < f(t)\}, \quad T \sim T_{n-1}$$

where f is the Student t density function for $n - 1$ degrees of freedom; and see Martin and Liu (2020) for more on this so-called maximum-specificity contour and optimal choices of $\pi(t)$ in other contexts.

For the final step we combine the plausibility contour for T with the association in (5) to derive a plausibility contour for Y^* . That is, given a predicted value y write $G_n^{-1}(y)$ for the solution in T to (5); then, the plausibility contour for Y^* is defined by $\pi_n(y) = \pi(G_n^{-1}(y))$. Since $\pi(T)$ satisfies (6) with equality it follows that $\pi(G_n^{-1}(Y^*))$ is a uniform random variable with respect to the joint distribution of $\{Y^n, Y^*\}$, and, therefore, the predictive plausibility contour is valid and efficient: for all $\alpha \in (0, 1)$

$$\sup_{\phi} P_{(Y^n, Y^*)|\phi}\{\pi_n(Y^*) \leq \alpha\} = \alpha,$$

and where $\phi = (\mu, \nu)$; see also Theorem 1 in Cella and Martin (2020).

For the above construction using the association in (5) and the optimal contour $\pi(t)$ the $100(1 - \alpha)\%$ prediction interval for Y^* is $C_\alpha(y^n) := \{y : \pi_n(y) > \alpha\}$ which may be written

$$\left\{ y : P_T \left(f(T) < f \left(\frac{y - \bar{Y}_n}{\sqrt{S^2(1 + 1/n)}} \right) \right) > \alpha \right\}.$$

Let $T_{m,\alpha}$ denote the α^{th} quantile of Student's t distribution with m degrees of freedom. Then, $\{z : P_T(f(T) < f(z)) > \alpha\}$ is simply $\{z : T_{n-1,\alpha/2} \leq z \leq T_{n-1,1-\alpha/2}\}$, and it follows that $C_\alpha(y^n)$ is equivalent to the interval

$$\bar{Y}_n \pm T_{n-1,1-\alpha/2} \sqrt{S^2(1 + 1/n)},$$

which is the classical exact prediction interval for Y^* (Fisher 1935) and the Bayesian prediction interval based on the default prior.

The IM framework may be unfamiliar to most readers, but as the above example shows, its inferences coincide with those of standard procedures. As we show in Section 5, the advantage of the IM framework is its ability to guarantee validity in more challenging situations for which standard methods fall short.

5 Valid IM predictions for random group effects

In this section we present an IM for predicting θ^* and \bar{Y}_k^* with respect to model (1). The first step of IM construction—the association step—is again the most challenging, and we devote considerable space in Section 5.1 to explaining it thoroughly; nevertheless, some technical details are deferred to the Appendices. The particular forms of the associations (given below in (11) and (13)) depend on whether the experiment is balanced, i.e., $n_i = n/I$, or unbalanced; and, unsurprisingly, the unbalanced case is more complicated. For valid predictions in unbalanced experiments we require the use of a local conditional

association—covered, e.g., in Chapter 6.5 of Martin and Liu (2015b)—along with a so-called *fused plausibility contour*, which we describe below in Section 5.2. A similar IM is provided in Martin and Liu (2015b) using a construction based on random sets and is used to make inferences on the variance components. We have modified that IM construction to follow the three-step construction laid out in Martin and Liu (2020) based on plausibility contours, and extended it to provide predictions for θ^* and \bar{Y}_k^* .

5.1 Association step

Begin with the data-generating equation in (1):

$$Y^n = \mu \mathbf{1} + (\sigma_a^2 Z Z^\top + \sigma^2 I_n)^{1/2} W,$$

where $W \sim N_n(0, I_n)$ and recall that $\theta^* \sim N(\mu, \sigma_a^2)$ and $\bar{Y}_k^* \sim N(\mu, \sigma_a^2 + \sigma^2/k)$. Our goal is to find reduced, one-dimensional associations for θ^* and \bar{Y}_k^* based on (1) and the minimal sufficient statistic for $(\mu, \sigma_a^2, \sigma^2)$ similar to the illustration in Section 4.

The minimal sufficient statistic for the variance components is a bit complicated. To start, make the one-to-one transformation $Y^n \mapsto (K^\top Y^n, \bar{Y}_n)$ where $\bar{Y}_n = \frac{1}{n} \mathbf{1}_{n \times 1}^\top Y^n$, and K is an $n \times (n-1)$ matrix such that $KK^\top = I_n - \frac{1}{n} \mathbf{1}\mathbf{1}^\top$ and $K^\top K = I_{n-1}$, the $n-1 \times 1$ identity matrix. Then,

$$\bar{Y}_n \sim N(\mu, V_0), \text{ where } V_0 = \left(\frac{\sigma^2}{n} + \frac{\sigma_a^2}{n^2} \sum_{i=1}^I n_i^2 \right). \quad (7)$$

Denote $G = K^\top Z Z^\top K$ and compute the diagonalizing matrix P such that $P^\top G P = \lambda I_{n-1}$ is equal to the identity matrix multiplied by the $(n-1) \times 1$ vector of eigenvalues of G , denoted λ . P may be written $P = [P_1, \dots, P_L]$ where L is the number of distinct eigenvalues of G and P_ℓ is an $(n-1) \times r_\ell$ matrix where r_ℓ is the multiplicity of λ_ℓ . Define $S_\ell = Y^\top K P_\ell P_\ell^\top K^\top Y$. Then, (S_1, \dots, S_L) are minimal sufficient for (σ_a^2, σ^2) and

$$S_\ell = (\lambda_\ell \sigma_a^2 + \sigma^2) V_\ell, \quad V_\ell \stackrel{ind.}{\sim} \chi^2(r_\ell), \quad \ell = 1, \dots, L. \quad (8)$$

Using (7) and (8) we can reduce the dimension of the association in (1) to $L+1$, obtaining the association

$$\begin{aligned} S_\ell &= (\lambda_\ell \sigma_a^2 + \sigma^2) V_\ell, \quad V_\ell \stackrel{ind.}{\sim} \chi^2(r_\ell), \quad \ell = 1, \dots, L; \\ \bar{Y}_n &= \mu + \left\{ \sigma_a^2 \frac{1}{n^2} \sum_{i=1}^I n_i^2 + \sigma^2 \frac{1}{n} \right\}^{1/2} Z_1, \end{aligned} \quad (9)$$

where Z_1 is independent of V_ℓ for $\ell = 1, \dots, L$. From (9) we can develop $(L+1)$ -dimensional associations for θ^* and for \bar{Y}_k^* . For θ^* , solve for μ in the second display in (9) and add α^* to each side, where $\alpha^* \sim N(0, \sigma_a^2)$ and α^* is independent of Y^n . For \bar{Y}_k^* , substitute the association for μ into the data-generating equation $\bar{Y}_k^* = \mu + (\sigma_a^2 + \sigma^2/k)^{1/2} Z_2$ where $Z_2 \sim N(0, 1)$ is independent of Z_1 and V_ℓ for $\ell = 1, \dots, L$. These two steps provide the

association

$$\begin{aligned}
S_\ell &= (\lambda_\ell \sigma_a^2 + \sigma^2) V_\ell, \quad V_\ell \stackrel{ind.}{\sim} \chi^2(r_\ell), \quad \ell = 1, \dots, L; \\
\theta^* &= \bar{Y}_n + \left\{ \sigma_a^2 \left(1 + \frac{1}{n^2} \sum_{i=1}^i n_i^2 \right) + \sigma^2 \frac{1}{n} \right\}^{1/2} Z_1, \\
\bar{Y}_k^* &= \bar{Y}_n + \left\{ \sigma_a^2 \left(1 + \frac{1}{n^2} \sum_{i=1}^i n_i^2 \right) + \sigma^2 \left(\frac{1}{n} + \frac{1}{k} \right) \right\}^{1/2} Z_2,
\end{aligned} \tag{10}$$

where $Z_2 \sim N(0, 1)$ is independent of Z_1 and V_ℓ for $\ell = 1, \dots, L$.

5.1.1 Balanced experiments

When the experimental design is balanced (meaning $n_i = n/I$ for $i = 1, \dots, I$), there are only $L = 2$ distinct eigenvalues of G and $\lambda_2 = 0$. In that case we can solve the association in (8) for (σ_a^2, σ^2) , yielding

$$\sigma^2 = S_2/V_2 \quad \text{and} \quad \sigma_a^2 = \lambda_1^{-1}(S_1/V_1 - S_2/V_2),$$

and substitute those solutions into the third display in (10) to obtain the following marginal one-dimensional association for \bar{Y}_k^* :

$$\begin{aligned}
\bar{Y}_k^* &= \bar{Y}_n + \left\{ \lambda_1^{-1}(S_1/V_1 - S_2/V_2) \left(1 + \frac{1}{n^2} \sum_{i=1}^i n_i^2 \right) \right. \\
&\quad \left. + (S_2/V_2) \left(\frac{1}{n} + \frac{1}{k} \right) \right\}^{1/2} Z_2
\end{aligned} \tag{11}$$

Since the right-hand side of (11) is one-dimensional and depends on no unknown parameters we have simplified the association as much as possible, so we take this as our final association for \bar{Y}_k^* balanced experiments. The final association for θ^* is the same as (11) with the omission of the $\frac{1}{k}$ factor of S_2/V_2 .

5.1.2 Unbalanced experiments

When the experimental design is unbalanced there are more than 2 distinct eigenvalues of G , so the association for (σ_a^2, σ^2) in (8) is overdetermined and further dimension reduction is needed in order to solve that association for a unique pair of variance components as we did in the balanced case. In these overdetermined cases in which we have already reduced dimension as far as possible using sufficiency, Martin and Liu (2015b) suggest further dimension reduction based on *localized conditioning*, which we describe next. The fact we have $L > 2$ equations in (8) each involving only one of L independent random variables V_ℓ for $\ell = 1, \dots, L$ and only two unknowns (σ_a^2, σ^2) implies an $(L - 2)$ -dimensional transformation of V_ℓ is actually observed; i.e., it is a statistic. Our goal is to rewrite the association as two parts: the $(L - 2)$ -dimensional statistic and the 2-dimensional unobserved random component. Then, we will condition on the observed component and use the remaining two-dimensional association to solve for (σ_a^2, σ^2) as we did in the balanced case.

For the different components of the association, consider a map from $V = (V_1, \dots, V_L)$ to $(\eta(V), \tau(V))$ where $\eta(V) = H(Y)$ denotes the $(L - 2)$ -dimensional observed feature of V equal to some statistic $H(Y)$ and $\tau(V)$ denotes the unobserved, 2-dimensional feature. A detailed construction of the map $V \mapsto (\eta(V), \tau(V))$ is given in Appendix A. An important aspect of the construction is that $\eta(V) := \eta(V, \sigma_{a_0}^2, \sigma_0^2)$ actually depends on (σ_a^2, σ^2) but this dependence vanishes when $(\sigma_a^2, \sigma^2) = (\sigma_{a_0}^2, \sigma_0^2)$ for any fixed, user-specified point $(\sigma_{a_0}^2, \sigma_0^2)$. Hence, the association formed by conditioning $\tau(V)$ on $\{V : \eta(V, \sigma_{a_0}^2, \sigma_0^2) = h\}$ is referred to as a *local conditional* association because $\eta(V, \sigma_{a_0}^2, \sigma_0^2)$ is locally fully observed, i.e., at the point $(\sigma_a^2, \sigma^2) = (\sigma_{a_0}^2, \sigma_0^2)$. Using this map given in Appendix A and conditioning on $\{V : \eta(V, \sigma_{a_0}^2, \sigma_0^2) = h\}$ we obtain the two-dimensional association

$$\begin{aligned} \sum_{\ell=1}^{L-1} \log S_\ell &= \sum_{\ell=1}^{L-1} \log(\lambda_\ell \sigma_a^2 + \sigma^2) + \Omega_1 \\ \log S_L &= \log \sigma^2 + \Omega_2, \end{aligned} \tag{12}$$

where $\Omega_i := \Omega_i((V, \sigma_{a_0}^2, \sigma_0^2))$ for $i = 1, 2$ denote random variables with the distributions of the components of $\tau(V)$ conditioned on $\{V : \eta(V, \sigma_{a_0}^2, \sigma_0^2) = h\}$. We can solve the system of equations in (12) for (σ_a^2, σ^2) using an iterative method, but the solutions are not available in closed form. For notational convenience we denote the solutions to (12) by $(\tilde{\sigma}_{a_0}^2, \tilde{\sigma}_0^2)$.

Plugging these solutions into the bottom display of the association in (9) we obtain the following local conditional association for \bar{Y}_k^* :

$$\begin{aligned} \bar{Y}_k^* &= \bar{Y}_n + \left\{ \tilde{\sigma}_{a_0}^2 \left(1 + \frac{1}{n^2} \sum_{i=1}^i n_i^2 \right) \right. \\ &\quad \left. + \tilde{\sigma}_0^2 \left(\frac{1}{n} + \frac{1}{k} \right) \right\}^{1/2} Z_2. \end{aligned} \tag{13}$$

The association for θ^* is equivalent to (13) with the omission of $\frac{1}{k}\sigma_0^2$. The above association, like (11), has minimal dimension and depends on no unknown parameters besides \bar{Y}_k^* . The difference between (11) and (13) is the latter's dependence on the localization point $(\sigma_{a_0}^2, \sigma_0^2)$. In the next step of the IM construction described in Section 5.2 we show that the association's dependence on $(\sigma_{a_0}^2, \sigma_0^2)$ does not compromise the predictive validity of the corresponding plausibility contours, but does increase the cost to compute the contours in practice.

5.1.3 The association for an existing group

When \bar{Y}_k^* represents the sample average of k future observations from an existing group, the associations in (11) and (13) must be modified to account for the correlation between \bar{Y}_k^* and Y^n . It is straightforward to account for the correlation between \bar{Y}_k^* and the sample mean \bar{Y}_n because they have a joint normal distribution parametrized by their correlation. On the other hand, the joint distribution of $(\bar{Y}_k^*, \bar{Y}_n, S_1, \dots, S_L)$ is very complicated. An approximate solution is to simply ignore the correlation between the future observations and the minimal sufficient statistics for the variance components. Doing so, we have the

following approximate association for balanced experiments in which the new observations come from group I ,

$$\bar{Y}_k^* = \bar{Y}_n + \left\{ \lambda_1^{-1}(S_1/V_1 - S_2/V_2) \left(1 - 2\frac{n_I}{n} + \frac{1}{n^2} \sum_{i=1}^i n_i^2 \right) + (S_2/V_2) \left(\frac{1}{n} + \frac{1}{k} \right) \right\}^{1/2} Z_2.$$

The only difference between the above association and (11) is that the “variance” term is decreased by $2\frac{n_I}{n}\lambda_1^{-1}(S_1/V_1 - S_2/V_2)$; for unbalanced experiments we make the analogous change to (13). Intuitively, the correlation between \bar{Y}_k^* and Y^n has the effect of sharpening the plausibility contour, and, hence, shortening prediction intervals. Therefore, we expect that ignoring the correlation between \bar{Y}_k^* and the (S_1, \dots, S_L) will have no effect on validity, but may cause the resulting IM to be less efficient. That seems to be the case in the simulation experiments in Section 6.

5.2 Predict and combine steps

The next step is to choose auxiliary plausibility contours for the auxiliary random variables in the associations (11) and (13). Below we provide the construction of plausibility contours for \bar{Y}_k^* ; the corresponding contours for θ^* are very similar and can be derived by making the obvious changes to the construction below. In the example in Section 4, the association in (5) is expressed as an invertible function of a Student t random variable, and we chose the maximum specificity contour $\pi(t) = P_T\{f(T) < t\}$ due to its optimality and the fact the auxiliary random variable T has a density available in closed-form. In principle, we could employ a similar technique for the associations in (11), but that strategy requires us to compute the marginal univariate density of the right-hand sides of those associations, which are complicated transformations of independent normal and χ^2 random variables. Fortunately, there is an alternative, simpler strategy useful when the auxiliary random variable has a complicated distribution. Rewrite the right-hand-side of the association in (11) as

$$\bar{Y}_k^* = F_n^{-1}(U), \quad U \sim \text{Unif}(0, 1), \quad (14)$$

where F_n denotes the cumulative distribution function of the random variable represented by the right-hand-side of (11). Since F_n is not available in closed-form, neither is F_n^{-1} , but the form of the association in (14) in terms of a uniform random variable is nonetheless helpful, because uniform random variables have known optimal plausibility contours. For a uniform auxiliary random variable on $[0, 1]$ the optimal plausibility contour satisfying (6) is the triangular contour given by

$$\pi(u) = 1 - 2|u - \frac{1}{2}|, \quad u \in [0, 1]; \quad (15)$$

and, see Martin and Liu (2020).

The last step is to combine the auxiliary plausibility contour $\pi(u)$ and the association in (14) to obtain the plausibility contour and function:

$$\pi_n(y) = \pi(F_n(y)) \quad \text{and} \quad \bar{\Pi}_n(A) = \sup_{y \in A} \pi_n(y). \quad (16)$$

Since F_n is not available in closed form we approximate it by Monte Carlo sampling; see Algorithm 1.

Algorithm 1: Monte Carlo approximation of $\pi_n(y)$

Choose a large integer $M > 0$;

for m in 1 to M **do**

 independently sample $V_{1,m} \sim \chi^2(r_1)$, $V_{2,m} \sim \chi^2(r_2)$, $Z_m \sim N(0, 1)$
 given the above samples, compute y_m according to (11).

end

Result: $\pi_n(y) \approx \pi(M^{-1} \#\{y_m \leq y\})$ for $\pi(\cdot)$ given in (15)

We suggest a similar strategy for unbalanced experiments corresponding to the association in (13). That association can be expressed as $\bar{Y}_k^* = F_n^{-1}(U)$ where $U \sim \text{Unif}(0, 1)$ and where F_n denotes the distribution function of the one-dimensional random variable given by the right-hand-side of (13), which depends on the localization point $(\sigma_{a_0}^2, \sigma_0^2)$. A similar Monte Carlo sampling strategy can be used to approximate the plausibility contour $\pi_n^{(\sigma_{a_0}^2, \sigma_0^2)}(y) = \pi(F_n(y))$ where π is the triangular auxiliary contour in (15); see Algorithm 2 below.

The contour $\pi_n^{(\sigma_{a_0}^2, \sigma_0^2)}(y)$ depends on the localization point $(\sigma_{a_0}^2, \sigma_0^2)$, so generally is not valid in the sense of (3) unless $(\sigma_{a_0}^2, \sigma_0^2)$ equal the true variance components. To ensure validity we define the plausibility contour π_n^f for \bar{Y}_k^* to be the pointwise supremum of local plausibility contours $\pi_n^{(\sigma_{a_0}^2, \sigma_0^2)}$ over all possible pairs of localization points:

$$\begin{aligned} \pi_n^f(y) &:= \sup_{(\sigma_{a_0}^2, \sigma_0^2)} \pi_n^{(\sigma_{a_0}^2, \sigma_0^2)}(y), \text{ and} \\ \bar{\Pi}_n^f(A) &:= \sup_{y \in A} \pi_n^f(y); \end{aligned} \tag{17}$$

and, see Proposition 2. The word ‘‘fusion’’ references the definition of a new plausibility contour as the pointwise supremum of a family of plausibility contours; hence the superscript f in $\pi_n^f(y)$, which stands for ‘‘fused’’ plausibility contour.

5.3 Validity of IM-based predictions

Predictive validity of the plausibility function $\bar{\Pi}_n(A)$ defined in (16) for balanced experiments follows from the general theory in Cella and Martin (2020); see their Theorem 1. As a consequence of Proposition 1, the $100(1 - \alpha)\%$ prediction interval defined by the α -cut of $\pi_n(y)$ is valid in the sense of (2); and, see Martin (2021) and their equations (10) and (11).

Proposition 1. *The plausibility function defined in (16) is valid in the sense of (3).*

Proof. The claim follows by checking the three sufficient conditions in Cella and Martin (2020) Theorem 1, appearing in their equations (13)–(15). The first condition requires that for all ϕ $\pi_n(\bar{Y}_k^*)$ is stochastically no smaller than a continuous uniform random variable on the interval $(0, 1)$ with respect to $P_{Y^n, \bar{Y}_k^* | \phi}$. By (14) and (15)

$$\pi_n(\bar{Y}_k^*) = \pi(U) = 1 - 2|U - \frac{1}{2}|, \quad U \sim \text{Unif}(0, 1).$$

Algorithm 2: Monte Carlo approximation of $\pi_n^f(y)$

Choose a J -dimensional grid of values $(\sigma_{a_0,j}^2, \sigma_{0,j}^2)$ for $j = 1, \dots, J$;

Choose a large integer $M > 0$;

for j in 1 to J **do**

for m in 1 to M **do**

 sample $\Omega_{1,m}(V, \sigma_{a_0,j}^2, \sigma_{0,j}^2)$ and $\Omega_{2,m}(V, \sigma_{a_0,j}^2, \sigma_{0,j}^2)$ by Markov chain Monte Carlo (MCMC) according to the densities given in Appendix A.

 solve the equations for (σ_a^2, σ^2) in (8) using the sampled values of $\Omega_{1,m}(V, \sigma_{a_0,j}^2, \sigma_{0,j}^2)$ and $\Omega_{2,m}(V, \sigma_{a_0,j}^2, \sigma_{0,j}^2)$, denoting the solutions by $\{\sigma_{a,m}^2(Y^n, \Omega_1, \sigma_{a_0,j}^2, \sigma_{0,j}^2), \sigma_m^2(Y^n, \Omega_2, \sigma_{a_0,j}^2, \sigma_{0,j}^2)\}$

 sample $Z_m \sim N(0, 1)$

 given the above samples, compute y_m^j according to (13).

end

Result: $\pi_n^{(\sigma_{a_0,j}^2, \sigma_{0,j}^2)}(y) \approx \pi(M^{-1} \#\{y_m^j \leq y\})$ for $\pi(\cdot)$ given in (15)

end

Result: $\pi_n^f(y) \approx \max_{j \in \{1, \dots, J\}} \pi_n^{(\sigma_{a_0,j}^2, \sigma_{0,j}^2)}(y)$

And, by straightforward calculation

$$P(1 - 2|U - \frac{1}{2}| \leq u) = u;$$

verifying the first condition. The second condition requires $\sup \pi_n(y) = 1$, which is satisfied because $\pi(u)$ has maximum of 1 occurring at $u = 1/2$. The third condition requires $\bar{\Pi}_n(A) := \sup_{y \in A} \pi_n(y)$, which is true by construction. \square

Validity of fused plausibility contours follows from Theorem 5 in Martin (2021); for more details see Section 4.2 of that paper.

Proposition 2. *The plausibility function defined in (17) is valid in the sense of (3).*

Proof. The proof proceeds by checking the two requirements of Theorem 5 in Martin (2021). First, we need $\sup_y \pi_n^f(y) = 1$, and this follows from the same argument as in the proof of Proposition 1 above. Next, define $\bar{\Pi}_n(A)^{(\sigma_{a_0}^2, \sigma_0^2)} := \sup_{y \in A} \pi_n^{(\sigma_{a_0}^2, \sigma_0^2)}(y)$. By the same argument as in the proof of Proposition 1, $\bar{\Pi}_n(A)^{(\sigma_{a_0}^2, \sigma_0^2)}$ is valid in the sense of (3) if $(\sigma_a^2, \sigma^2) = (\sigma_{a_0}^2, \sigma_0^2)$, and this satisfies the second requirement of Theorem 5 in Martin (2021). \square

In practice, computing the plausibility contours relies on Monte Carlo, and, in the case of the fused plausibility contour, MCMC and a two-dimensional grid search. As a result, predictive validity only holds approximately, but we emphasize the quality of this approximation is entirely user-controlled since it depends only on the number M of Monte Carlo/MCMC samples used and the fineness of the grid, determined by J , but not on the sample size. In the simulation experiments we investigate in Section 6 we find the plausibility contours computed by Algorithms 1 and 2 achieve validity based on modest numbers of Monte Carlo samples and only a rough grid search.

6 Simulations

We consider the following twelve scenarios in a simulation study aimed at examining frequentist coverage probability of prediction intervals for θ^* using several methods. We include additional comparisons of prediction intervals for a new response Y^* in Appendix B. In each setting we fix $\mu = 0$ and vary the values of variance components over four pairs $(\sigma_a^2, \sigma^2) = (0.01, 1.0), (0.1, 1.0), (0.5, 0.5),$ and $(1.0, 0.1)$. Recall, several authors report Student's t -based prediction intervals perform poorly when the between-group variance σ_a^2 is small. Our four designs include:

- A. Balanced, small study with 5 groups of 6 observations each.
- B. Balanced, medium-sized study with 10 groups of 12 observations each.
- C. Unbalanced, small study with 3 groups of 4 observations, 1 group with 6 observations, and 1 group with 12 observations.
- D. Unbalanced, medium-sized study with 10 groups of the following sizes: 4, 4, 7, 11, 13, 16, 16, 16, 16, and 17.

We compare our IM prediction intervals to six other methods:

- i) *Oracle* method prediction intervals are based on the true values of the variance components and the association in (10). The $100(1 - \alpha)\%$ oracle prediction interval for θ^* has endpoints

$$\bar{y}_n \pm \left\{ \sigma_a^2 \left(1 + \frac{1}{n^2} \sum_{i=1}^i n_i^2 \right) + \sigma^2 \frac{1}{n} \right\}^{1/2} z_{1-\alpha/2}$$

where z_α is the lower $100\alpha\%$ standard normal quantile and \bar{y}_n is the sample mean of observed responses.

- ii) *Student t* prediction intervals are also based on the association in (10), but with the variance components replaced by their maximum likelihood estimates, and the normal distribution quantiles replaced by quantiles of a Student t distribution with $I - 2$ degrees of freedom; this is the frequentist method suggested by Higgins et al. (2009).
- iii) *IM* prediction intervals are computed using Algorithms 1 and 2 as described in Section 5. In each iteration of those algorithms we use $M = 10000$ Monte Carlo/MCMC samples. When using Algorithm 2 we use an equally-spaced grid on $[0.05, 2] \times [0.05, 2]$ of $J = 25$ pairs of points.
- iv) *Conformal* prediction intervals are based on the non-conformity measure $T_n(\vartheta) = |\vartheta - \bar{Y}_n|$. Compute the I non-conformity values $T_i(\vartheta) = \left| \bar{y}_i - \frac{1}{I} \left\{ \vartheta + \sum_{\ell \neq i} \bar{y}_\ell \right\} \right|$ for $i = 1, \dots, I$. The plausibility of $\{\theta^* = \vartheta\}$ is given by $\pi_n^c(y) = I^{-1} \#\{T_i(\vartheta) > T_n(\vartheta)\}$. A $100 \left(1 - \frac{I\alpha}{I} \right) \%$ conformal prediction interval for \bar{Y}_1^* is given by the set $\{\vartheta : \pi_n^c(\vartheta) \geq \frac{I\alpha}{I}\}$.

- v) *Nonparametric bootstrap* prediction intervals for θ^* are computed using the percentile method and stratified resampling. To compute the bootstrap distribution of the within-group means we sample with replacement within each group sample and return the bootstrapped within-trial sample means. A $100(1 - \alpha)\%$ prediction interval for a new group mean is defined by the $\alpha/2$ and $1 - \alpha/2$ quantiles of this bootstrap distribution.
- vi) *Parametric bootstrap* prediction intervals for θ^* are computed using the association in (10) with the variance components replaced by their parametric bootstrap-based estimates. Specifically, we randomly sample parametric bootstrap responses $y^{n,b} = (y_{11}^b, \dots, y_{I n_i}^b)^\top$ according to (1) with the variance components replaced by their MLEs based on the original data y^n . Then, we compute new MLEs based on $y^{n,b}$ and sample $\theta^{*,b} \sim N(\bar{y}^{n,b}, \sigma_a^{2,b})$. Repeat for $b = 1, \dots, B$ times and define a $100(1 - \alpha)\%$ prediction interval for a new group mean by the $\alpha/2$ and $1 - \alpha/2$ quantiles of the values $(\theta^{*,1}, \dots, \theta^{*,B})$.
- vii) *Bayesian* prediction intervals for θ^* are computed using the R package `brms` and the function `posterior_epred`; see Bürkner (2017). This function computes draws of the mean of the posterior predictive distribution of a new group. We use a normal distribution prior with mean zero and standard deviation 4 for μ , and independent half-Cauchy prior distributions with scale parameter equal to 1 for the variance components.

Concerning the methods for constructing prediction described above we make a few clarifying remarks. For the nonparametric bootstrap we also tried a hierarchical bootstrap procedure in which we resampled groups as well as responses within groups. The corresponding prediction intervals for θ^* were not substantially different than those based on the stratified bootstrap. The conformal method can be interpreted as a nonparametric IM, and satisfies predictive validity no matter the underlying data distribution; see Cella and Martin (2020). One down-side of the conformal method is that because it is a discrete method, its available coverage levels for θ^* are fractions of I , which limits its usefulness when the number of groups is small.

Table 1 provides results of our simulation study for predicting a new group mean θ^* . The nominal coverage of oracle, Student’s t , IM, and bootstrap intervals displayed in Table 2 is 95%. The conformal method—like other discrete methods, e.g., confidence intervals for a binomial proportion—has a limited range of nominal coverage levels. Its nominal coverage is about 80% for simulation settings B and D and lower for A and C, but in practice actual coverage is considerably higher. Besides the 95% intervals summarized in Table 1 we compared prediction intervals over a wide range of coverage levels; see Figures 3 and 4 in the Appendix. We would like to highlight three main take-away messages from our simulation study:

1. As claimed, the IM method is valid over all simulations and for any nominal coverage level. When the true between-group variance is nearly zero the IM method is inefficient, but in all other cases its efficiency is similar to the Student t intervals when the latter have adequate coverage.
2. The Student t -based intervals are often shorter than the Oracle intervals and under-cover. Figure 3 in the Appendix shows their under-coverage is not dependent upon

the chosen nominal level. When the between-group variance is close to zero its (restricted) maximum likelihood estimate is often very close to zero, and the Student t prediction intervals undercover substantially in those cases. For example, in setting B with $(\sigma_a^2, \sigma^2) = (0.1, 1.0)$ about 86% of simulated MLEs $\hat{\sigma}_a^2$ were less than 0.0001; and, see Figure 4 in the Appendix. The performance of Student’s t -based intervals did not necessarily improve with increased sample size; compare settings A to B and C to D for $(\sigma_a^2, \sigma^2) = (0.1, 1.0)$.

3. Since the Student’s t -based prediction intervals apparently do not adequately account for the uncertainty in predicting θ^* it is reasonable to try other methods. Perhaps surprisingly, common techniques like (nonparametric or parametric) bootstrap and Bayesian methods also fail to generate valid prediction intervals, even in many cases where the Student’s t -based prediction intervals are adequate.

Appendix B includes simulation results for predicting a new response Y^* for both a new and an existing group using the same simulation settings. To summarize, the IM method performs best out of all the prediction methods both in terms of validity and efficiency. The Student’s t -based prediction intervals for Y^* are much less efficient than the IM prediction intervals, but do not suffer under-coverage in any of our settings as they did for predicting θ^* . The bootstrap and Bayes methods, on the other hand, continue to under-cover in several settings.

7 Soybean yield and fungicide use in Iowa

In this section we analyze soybean yields from 37 Iowa farms comparing the effect of fungicide use on yield versus current growing practices. The experimental data is unbalanced, with farms using Stratego fungicide on between 3 and 12 strips, and contains a total of 200 observations on the natural logarithm of yield proportions (log of response ratio) for pairs of treated versus non-treated strips; and see Laurent et al. (2020).

Figure 1 displays ranges of fungicide effects across the farms and provides some sense of the relative magnitudes of between- and within-farm variance. Within-farm variance is larger than between-farm variance, but it may be surprising just how small the between-farm variance is estimated to be. The R function `lmer` from the widely-used `lme4` package Bates et al. (2015) fits the model and displays a warning message “boundary (singular) fit”, which, in this case, means the estimated between-farm variance is essentially zero.

We compute prediction intervals for θ^* and for a single new response Y^* from a new group using the Student t , IM, conformal, non-parametric bootstrap, parametric bootstrap, and Bayesian methods used in Section 6. Table 2 provides 95% prediction intervals for a new farm mean effect θ^* and a single new response Y^* from a new farm for these six methods. The takeaway message here is that the Student- t method for predicting θ^* looks like an outlier. Our simulation results in Section 6 showed these prediction intervals are generally too short and undercover when the estimated between-group variance is small. And, for this data, the Student- t method again produces a very narrow prediction interval for θ^* . Of the four parametric methods used, the Student- t interval for θ^* is by far the shortest while the IM interval is most conservative. The parametric bootstrap and Bayesian methods perform similarly, with lengths in between

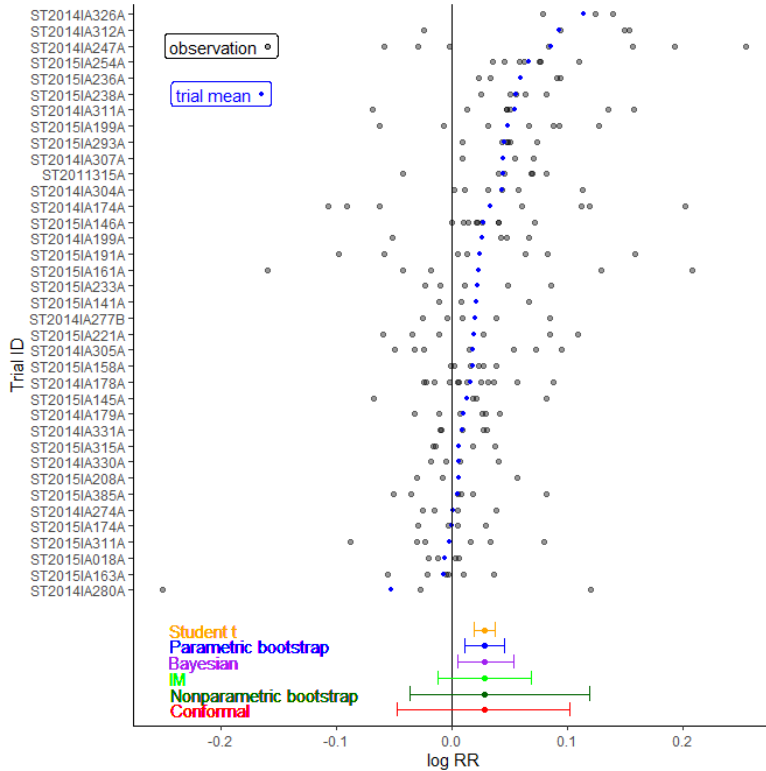
Table 1: Observed coverage proportion and ratios of average prediction interval lengths compared to the Oracle method of 95% prediction intervals for θ^* . Gray highlighting denotes significant under-coverage (excluding conformal method).

		Simulation Setting							
		A		B		C		D	
(σ_a^2, σ^2)	Method	Coverage	Length	Coverage	Length	Coverage	Length	Coverage	Length
(0.01, 1.0)	Oracle	0.94	—	0.96	—	0.94	—	0.96	—
	Student t	0.99	1.83	0.94	1.20	0.99	1.80	0.94	1.20
	IM	1.00	2.99	1.00	2.09	1.00	3.36	1.00	2.69
	Conformal	0.97	2.05	1.00	9.36	0.97	2.19	1.00	8.15
	Nonpar. Boot.	1.00	2.41	1.00	2.82	1.00	2.57	1.00	3.27
	Para. Boot.	1.00	2.00	1.00	1.67	1.00	2.05	1.00	1.69
	Bayes	1.00	1.76	0.99	1.56	1.00	1.84	1.00	1.62
(0.1, 1.0)	Oracle	0.94	—	0.95	—	0.94	—	0.95	—
	Student t	0.92	1.35	0.86	1.00	0.91	1.28	0.85	0.99
	IM	1.00	1.89	0.96	1.24	1.00	2.01	0.97	1.33
	Conformal	0.92	1.31	0.97	3.50	0.93	1.33	0.98	3.18
	Nonpar. Boot.	0.99	1.44	0.99	1.38	0.98	1.50	0.99	1.53
	Para. Boot.	0.95	1.33	0.92	1.08	0.95	1.33	0.93	1.09
	Bayes	0.94	1.11	0.90	0.96	0.95	1.13	0.91	0.98
(0.5, 0.5)	Oracle	0.94	—	0.95	—	0.94	—	0.94	—
	Student t	0.91	1.34	0.93	1.08	0.90	1.31	0.94	1.08
	IM	0.95	1.34	0.94	1.11	0.95	1.42	0.94	1.12
	Conformal	0.84	0.92	0.92	1.58	0.86	0.90	0.93	1.64
	Nonpar. Boot.	0.82	0.80	0.89	0.88	0.85	0.80	0.90	0.90
	Para. Boot.	0.88	1.07	0.93	1.03	0.89	1.06	0.92	1.03
	Bayes	0.79	0.74	0.86	0.83	0.81	0.73	0.87	0.83
(1.0, 0.1)	Oracle	0.95	—	0.94	—	0.94	—	0.94	—
	Student t	0.95	1.38	0.94	1.09	0.95	1.37	0.94	1.09
	IM	0.93	1.27	0.94	1.11	0.95	1.40	0.95	1.19
	Conformal	0.82	0.85	0.91	1.29	0.82	0.83	0.92	1.29
	Nonpar. Boot.	0.72	0.61	0.84	0.78	0.72	0.61	0.84	0.78
	Para. Boot.	0.89	1.05	0.93	1.03	0.90	1.05	0.93	1.03
	Bayes	0.72	0.61	0.84	0.78	0.72	0.61	0.84	0.77

those other two methods. The nonparametric methods produce very similar intervals, both much wider than any of the parametric methods. On the other hand, for predicting a new response, the IM method produces the shortest interval while the other methods all produce very similar, wider prediction intervals. That is a bit surprising because the IM method did not, on average, produce the shortest prediction intervals for Y^* in any of our simulations.

Figure 2 displays the fused plausibility contour $\pi_n^f(\vartheta)$ for a new group mean fungicide effect θ^* . The fused contour corresponds to the outer black curve in the figure. The gray area corresponds to local plausibility contours $\pi_n^{(\sigma_a^2, \sigma_0^2)}(\vartheta)$ over a equally-spaced grid of 400 pairs of variance component values in the region $[0.0001, 4] \times [0.0001, 4]$. Several useful summaries can be deduced from the contour plot. The peak of the fused contour occurs at the sample mean effect of 0.028. 100(1 - α)% prediction intervals for θ^* may be read off of the fused contour by making horizontal cuts at height α . And, since the contour peaks to the right of zero, the plausibility of $\{\theta^* \leq 0\}$ equals $\pi_n^f(0) \approx 0.132$, which is not negligible.

Figure 1: Responses and mean responses over 37 Iowa farms. Prediction intervals for a new farm mean response using six different methods are displayed at the bottom of the figure.



8 Discussion

Recently, researchers and statistics practitioners have recognized that valid statistical predictive inference lags behind developments in population-level inference, even in relatively simple models. This presents an opportunity for statisticians to develop methods to help practitioners better answer relevant questions about experiments requiring predictions at the group or individual level. We think the present paper illustrates predictive inference using IMs is both valid and practical to implement.

An important aspect of the IM approach is its leveraging of minimal sufficient statistics, which may go unreported in meta-analysis applications. Our approach highlights that one benefit of more complete data-sharing is improved prediction and inference, and we hope this persuades researchers to consider making their data publicly available.

Besides the current application to a one-way Gaussian random effects model, the proposed methods can be extended to more general Gaussian linear mixed models. Research on IMs and IM-based prediction is on-going and developments for more complicated models and settings are underway, including in supervised learning and nonparametrics, e.g., estimating equation models; see Cella and Martin (2021a) and Cella and Martin (2021b).

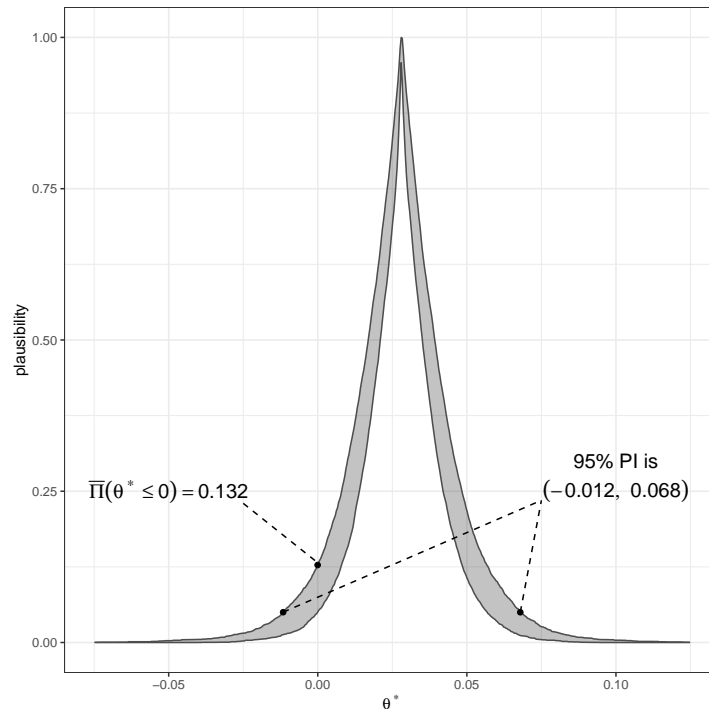
Table 2: 95% prediction intervals for θ^* and a single new response Y^* on soybean yield for the data described in Section 7.

Method	95% Prediction Intervals	
	θ^*	Y^*
Student t	(0.019, 0.037)	(−0.096, 0.152)
Para. Boot.	(0.007, 0.049)	(−0.094, 0.150)
Bayesian	(0.005, 0.055)	(−0.098, 0.152)
IM	(−0.012, 0.068)	(−0.054, 0.110)
Nonpar. Boot.	(−0.037, 0.119)	(−0.082, 0.162)
Conformal	(−0.048, 0.102)	(−0.097, 0.153)

References

- Altman, N., and Krzywinski, M. (2018). Predicting with confidence and tolerance. *Nat. Methods* 15:841–845.
- Altman, N., and Krzywinski, M. (2013). Error bars. *Nat. Methods* 10(10):921–922.
- Balasubramanian, V., Ho, S., and Vovk, V. (2014). Conformal Prediction for Reliable Machine Learning: Theory, Adaptations and Applications. Elsevier Science.
- Bates, D., Mächler, M., Bolker, B., and Walker, S. (2015). Fitting Linear Mixed-Effects Models Using lme4. *J. Stat. Softw.* 67(1):1–48.
- Bürkner, P.-C. (2017). brms: An R Package for Bayesian Multilevel Models Using Stan. *J. Stat. Softw.* 80(1):1–28.
- Cella, L. and Martin, R. (2020). Strong validity, consonance, and conformal prediction. <https://arxiv.org/abs/2001.09225v2>.
- Cella, L. and Martin, R. (2021). Valid inferential models for prediction in supervised learning problems. Proceedings of the Twelveth International Symposium on Imprecise Probability: Theories and Applications, PMLR 147:72-82.
- Cella, L. and Martin, R. (2021). Approximately valid probabilistic inference on a class of statistical functionals. <https://arxiv.org/abs/2112.10232v1>.
- Fisher, R. A. (1935). The fiducial argument in statistical inference. *Ann. Eugen.* 6:391–398.
- Higgins J. P. T., Thompson, S. G., and Spiegelhalter, D. J. (2009). A re-evaluation of random-effects meta-analysis. *J. R. Statist. Soc. A* 172: 137–159.
- Inthout, J., Ioannidis, J. P. A., Rovers, M. M., and Goeman, J. J. (2016). Plea for routinely presenting prediction intervals in meta-analysis. *BMJ Open* 6:e010247. doi: 10.1136/bmjopen-2015-010247

Figure 2: Fused plausibility contour π_n^f (black outer curve) along with local plausibility contours $\pi_n^{(\sigma_{a0}^2, \sigma_0^2)}$ over grid of variance component values (grey fill) for a new farm mean fungicide effect θ^* for the data in Section 7.



Laurent, A., Miguez, F., Kyverga, P., and Makowski, D. (2020). Going beyond mean effect size: Presenting prediction intervals for on-farm network trial analyses. *Eur. J. Agron.* 120: 126127.

Martin, R. (2021). An imprecise-probabilistic characterization of frequentist statistical inference. <https://arxiv.org/abs/2112.10904v1>

Martin, R. and Lingham, R. (2016). Prior-free probabilistic prediction of future observations. *Technometrics* 58:(2) 225–235.

Martin, R. and Liu, C. (2015a). Conditional inferential models: combining information for prior-free probabilistic inference. *J. R. Stat. Soc. Series B.* 77: 195–217.

Martin, R. and Liu, C. (2015b). *Inferential Models: Reasoning with Uncertainty*. Monographs in Statistics and Applied Probability Series, Chapman & Hall/CRC Press.

Martin, R. and Liu, C. (2020). Inferential models and possibility measures. <https://arxiv.org/abs/2008.06874v2>.

Partlett, C. and Riley, R. D. (2016) Random effects meta-analysis: Coverage performance of 95% confidence and prediction intervals following REML estimation. *Stat. Med.* 36: 301–317.

A Details for the association step in Section 5.1.2

The method described in this section can be found in Sections 6.3.2 and 6.5 of Martin and Liu (2015b) and Section 6.5 of Martin and Liu (2015a).

Solve the association equations in (8) of the paper for the auxiliary random variables V_ℓ to find

$$V_\ell = \frac{S_\ell}{\lambda_\ell \sigma_a^2 + \sigma^2}, \quad \ell = 1, \dots, L-1, \quad V_L = \frac{S_L}{\sigma^2}.$$

The idea is to find a function of $V = (V_1, \dots, V_L)$ denoted $\eta(V)$ that is insensitive to changes in (σ_a^2, σ^2) . Such a function η is, essentially, observed, and while it may not technically satisfy the statistical definition of ancillarity, it makes sense to condition inference for variance components on η . To find η we look for a function such that its partial derivatives with respect to (σ_a^2, σ^2) vanish.

The partial derivatives of V_ℓ with respect to (σ_a^2, σ^2) are given by $\text{diag}(V_\ell)W(\sigma_a^2, \sigma^2)$ where the $L \times 2$ matrix $W(\sigma_a^2, \sigma^2)$ with rows w_ℓ is given by

$$w_\ell(\sigma_a^2, \sigma^2) = \left(-\frac{\lambda_\ell}{\lambda_\ell \sigma_a^2 + \sigma^2}, -\frac{1}{\lambda_\ell \sigma_a^2 + \sigma^2} \right), \quad \ell = 1, \dots, L-1,$$

$$w_L(\sigma_a^2, \sigma^2) = (0, -\sigma^{-2}).$$

Unfortunately, we are not able to find a function with everywhere vanishing derivatives. But, we can define a function $\eta_{\sigma_{a_0}^2, \sigma_0^2}(v)$ such that its partial derivatives in (σ_a^2, σ^2) vanish at the given pair $(\sigma_{a_0}^2, \sigma_0^2)$. To see this, choose arbitrary, positive values $(\sigma_{a_0}^2, \sigma_0^2)$, and define

$$\eta_{\sigma_{a_0}^2, \sigma_0^2}(v) = (\log v_1, \dots, \log v_L) \Pi(\sigma_{a_0}^2, \sigma_0^2)^\top$$

where $v = (v_1, \dots, v_L)$ is a realization of the random variables V_1, \dots, V_L defined in (8) and $\Pi(\sigma_{a_0}^2, \sigma_0^2)$ is a $(L-2) \times L$ matrix with rows orthogonal to the columns of $W(\sigma_{a_0}^2, \sigma_0^2)$. To determine $\Pi(\sigma_{a_0}^2, \sigma_0^2)$ solve the homogeneous equation $W^\top x = 0$ for an $L \times 1$ vector x . Since W^\top has rank strictly less than L there are infinitely many solutions, and any $L-2$ of these may be taken to form the rows of $\Pi(\sigma_{a_0}^2, \sigma_0^2)$. The point of this construction is that

$$\frac{\partial \eta_{\sigma_{a_0}^2, \sigma_0^2}(V)}{\partial V} \cdot \frac{\partial V}{\partial (\sigma_{a_0}^2, \sigma_0^2)} = 0_{(L-2) \times 2},$$

so that the function $\eta_{\sigma_{a_0}^2, \sigma_0^2}(V) = H_{\sigma_{a_0}^2, \sigma_0^2}(S)$ is observed, where

$$H_{\sigma_{a_0}^2, \sigma_0^2}(S)^\top = \left(\log \frac{S_1}{\lambda_1 \sigma_{a_0}^2 + \sigma_0^2}, \dots, \right.$$

$$\left. \log \frac{S_{L-1}}{\lambda_{L-1} \sigma_{a_0}^2 + \sigma_0^2}, \log \frac{S_L}{\sigma_0^2} \right) \Pi(\sigma_{a_0}^2, \sigma_0^2)^\top.$$

This allows us to condition on the observed value $H_{\sigma_{a_0}^2, \sigma_0^2}(S)$ and form a conditional association of $\tau(V)$ given $\eta_{\sigma_{a_0}^2, \sigma_0^2}(V) = H_{\sigma_{a_0}^2, \sigma_0^2}(S)$ where

$$\begin{pmatrix} \eta_{\sigma_{a_0}^2, \sigma_0^2}(v) \\ \tau(v) \end{pmatrix} = \begin{pmatrix} \Pi(\sigma_{a_0}^2, \sigma_0^2) \\ 1 \cdots 1 0 \\ 0 \cdots 0 1 \end{pmatrix} \begin{pmatrix} \log v_1 \\ \vdots \\ \log v_L \end{pmatrix}. \quad (18)$$

Taking the logarithm on both sides of each equation in (8) the two-dimensional conditional association can be written

$$\sum_{\ell=1}^{L-1} \log S_{\ell} = \sum_{\ell=1}^{L-1} \log(\lambda_{\ell} \sigma_a^2 + \sigma^2) + \Omega_1$$

$$\log S_L = \log \sigma^2 + \Omega_2$$

where (Ω_1, Ω_2) has the same joint distribution as $\tau(V)$ conditioned on $\{V : \eta(V, \sigma_{a0}^2, \sigma_0^2) = h\}$. This is the association appearing in (12) of the paper.

The marginal density $f_{\ell}(v)$ of $\log V_{\ell}$ is proportional to $\exp\{\frac{1}{2}r_{\ell}v - \frac{1}{2}\exp(v)\}$, and, by independence, the joint density of $\log V$ is the product $\prod_{\ell=1}^L f_{\ell}(v)$. Let A denote the $L \times L$ matrix on the right-hand side of (18). Then, the joint density of $U = (\eta_{\sigma_{a0}^2, \sigma_0^2}, \tau(v))$ is proportional to $\prod_{\ell=1}^L f_{\ell}[A^{-1}u]_{\ell}$. The conditional density of $\tau(V)$ given $\eta_{\sigma_{a0}^2, \sigma_0^2}(V) = H_{\sigma_{a0}^2, \sigma_0^2}(S)$ (which is the joint density of (Ω_1, Ω_2)) is proportional to this joint density with $(u_1, \dots, u_{L-2}) = H_{\sigma_{a0}^2, \sigma_0^2}(S)$. Given this joint density we can apply standard Markov chain Monte Carlo methods to sample (Ω_1, Ω_2) as required by Algorithm 2; see the codes available at <https://github.com/nasyring/impred>.

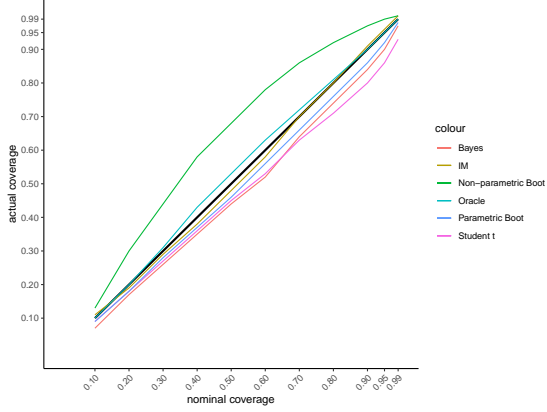
B Further Simulation Results

Figures 1 and 2 below supplement Table 1 in the paper. Figure 1 panel (a) illustrates that the under-coverage issues, particularly with respect to Student's t -based prediction intervals, are consistent over all nominal coverage levels. The IM-based intervals, in contrast, are consistently valid. Figure 1 panel (b) shows that under-coverage is associated with prediction intervals that are too short. Figure 2 suggests that when the true between-group variance is small relative to within-group variance, underestimation of between-group variance leads to under-coverage of prediction intervals. This issue is most pronounced for Student's t -based intervals, and this simulation agrees with the behavior of these intervals reported in Inthout et al. (2016); Laurent et al. (2020); Partlett and Riley (2016).

In addition to the results reported in Section 6 we also evaluated the performance of those methods for predicting new responses, both for a new and an existing group; see Tables 3 and 4 below. Similar to the simulations for predicting a new group mean, the IM method consistently attains or exceeds its nominal coverage level. The Student t intervals perform better with respect to coverage level for new responses compared to a new group mean, but are less efficient than the IM intervals. Again, the bootstrap and Bayesian prediction intervals often fail to cover at the nominal level when predicting a response from a new group, but fare better at predicting a new response from an existing group. This behavior suggests these methods underestimate sampling variability at the group level.

Figure 3: Results of simulation setting B with $(\sigma_a^2, \sigma^2) = (0.1, 1.0)$.

(a) Observed coverage proportions of prediction intervals.



(b) Observed ratios of average prediction interval lengths compared to the Oracle method.

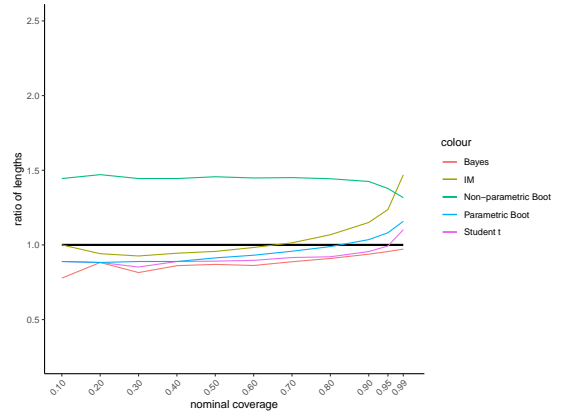
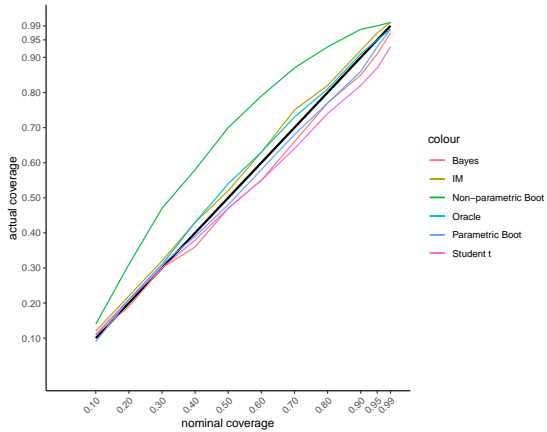


Figure 4: Observed coverage proportions for simulation setting B with $(\sigma_a^2, \sigma^2) = (0.1, 1.0)$.

(a) Subset of simulations in which $\hat{\sigma}_a^2 > 0.0001$.



(b) Subset of simulations in which $\hat{\sigma}_a^2 \leq 0.0001$.

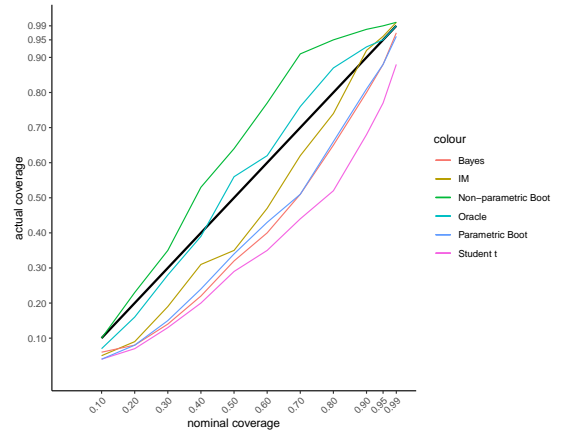


Table 3: Observed coverage proportion and ratios of average prediction interval lengths compared to the Oracle method of 95% prediction intervals for a new observation Y^* in a new group. Gray highlighting denotes significant under-coverage.

		Simulation Setting							
(σ_a^2, σ^2)	Method	A		B		C		D	
		Coverage	Length	Coverage	Length	Coverage	Length	Coverage	Length
(0.01, 1.0)	Oracle	0.96	—	0.96	—	0.96	—	0.96	—
	Student t	1.00	1.58	0.98	1.17	1.00	1.59	0.98	1.17
	IM	0.98	1.17	0.97	1.05	0.99	1.25	0.97	1.11
	Conformal	0.91	0.88	0.92	0.85	0.90	0.88	0.91	0.85
	Nonpar. Boot.	0.94	1.01	0.95	0.99	0.94	1.00	0.95	0.99
	Para. Boot.	0.95	1.02	0.95	0.99	0.96	1.03	0.96	1.00
	Bayes	0.96	1.07	0.96	1.02	0.96	1.08	0.96	1.02
(0.1, 1.0)	Oracle	0.95	—	0.96	—	0.96	—	0.96	—
	Student t	1.00	1.57	0.98	1.17	1.00	1.57	0.98	1.17
	IM	0.98	1.18	0.96	1.05	0.99	1.23	0.97	1.07
	Conformal	0.90	0.87	0.91	0.84	0.89	0.86	0.91	0.84
	Nonpar. Boot.	0.92	1.00	0.94	0.98	0.92	0.99	0.94	0.98
	Para. Boot.	0.95	1.02	0.95	1.00	0.95	1.02	0.96	1.00
	Bayes	0.96	1.05	0.96	1.01	0.96	1.06	0.96	1.01
(0.5, 0.5)	Oracle	0.95	—	0.95	—	0.95	—	0.95	—
	Student t	0.99	1.50	0.97	1.14	0.99	1.49	0.97	1.14
	IM	0.96	1.23	0.96	1.08	0.97	1.27	0.96	1.08
	Conformal	0.85	0.80	0.88	0.81	0.84	0.78	0.87	0.80
	Nonpar. Boot.	0.88	0.90	0.92	0.93	0.88	0.88	0.91	0.93
	Para. Boot.	0.92	1.04	0.94	1.01	0.93	1.03	0.94	1.01
	Bayes	0.91	0.93	0.92	0.95	0.92	0.92	0.93	0.95
(1.0, 0.1)	Oracle	0.94	—	0.94	—	0.94	—	0.94	—
	Student t	0.96	1.41	0.94	1.10	0.97	1.40	0.94	1.10
	IM	0.94	1.25	0.94	1.10	0.96	1.37	0.94	1.17
	Conformal	0.78	0.71	0.84	0.78	0.76	0.69	0.82	0.75
	Nonpar. Boot.	0.78	0.71	0.87	0.83	0.75	0.69	0.86	0.82
	Para. Boot.	0.90	1.05	0.92	1.02	0.90	1.04	0.93	1.02
	Bayes	0.78	0.72	0.88	0.84	0.78	0.70	0.87	0.84

Table 4: Observed coverage proportion and ratios of average prediction interval lengths compared to the Oracle method of 95% prediction intervals for a new observation Y^* in an existing group.

		Simulation Setting							
		A		B		C		D	
(σ_a^2, σ^2)	Method	Coverage	Length	Coverage	Length	Coverage	Length	Coverage	Length
(0.01, 1.0)	Oracle	0.94	—	0.95	—	0.94	—	0.95	—
	Student t	1.00	1.59	0.97	1.17	1.00	1.59	0.97	1.17
	IM	0.96	1.11	0.96	1.05	0.96	1.12	0.96	1.10
	Conformal	0.88	0.97	0.92	1.09	0.94	1.08	0.94	1.10
	Para. Boot.	0.94	1.00	0.94	1.00	0.94	0.99	0.94	0.99
	Bayes	0.95	1.06	0.95	1.02	0.95	1.05	0.95	1.02
(0.1, 1.0)	Oracle	0.95	—	0.94	—	0.95	—	0.95	—
	Student t	0.99	1.60	0.97	1.18	1.00	1.62	0.97	1.18
	IM	0.97	1.12	0.96	1.05	0.96	1.09	0.96	1.06
	Conformal	0.88	0.93	0.92	1.05	0.94	1.06	0.94	1.06
	Para. Boot.	0.95	1.01	0.95	1.00	0.94	1.00	0.94	1.00
	Bayes	0.96	1.04	0.95	0.99	0.96	1.04	0.96	0.99
(0.5, 0.5)	Oracle	0.95	—	0.96	—	0.95	—	0.96	—
	Student t	1.00	1.66	0.98	1.19	1.00	1.85	0.98	1.22
	IM	0.97	1.17	0.97	1.07	0.96	1.07	0.97	1.07
	Conformal	0.88	0.76	0.92	0.84	0.94	0.95	0.94	0.82
	Para. Boot.	0.96	1.05	0.96	1.02	0.94	1.06	0.96	1.02
	Bayes	0.95	0.84	0.94	0.76	0.96	0.91	0.95	0.77
(1.0, 0.1)	Oracle	0.96	—	0.96	—	0.96	—	0.96	—
	Student t	1.00	1.69	0.98	1.20	1.00	2.19	0.97	1.25
	IM	1.00	1.20	0.98	1.09	0.97	1.22	0.97	1.16
	Conformal	0.88	0.47	0.92	0.51	0.94	0.70	0.94	0.38
	Para. Boot.	0.98	1.08	0.97	1.03	0.95	1.13	0.96	1.03
	Bayes	0.95	0.38	0.95	0.33	0.96	0.47	0.95	0.34